

Design Modification and Finite Element Analysis of Stainless Steel 316L Locking Compression Plates for Mid-Transverse Fractures

*Muhammad Naufal bin Nazeri, Solehuddin Shuib**
School of Mechanical Engineering, College of Engineering,
Universiti Teknologi MARA, Shah Alam, 40450, Selangor, MALAYSIA
*solehuddin2455@uitm.edu.my

Ahmad Zafir Romli
Faculty of Applied Sciences, Universiti Teknologi MARA, 40450, Shah Alam,
Selangor, MALAYSIA

Mohd Fairudz Mohd Miswan
Faculty of Medicine, Universiti Teknologi MARA, Sungai Buloh Campus,
Selangor Branch, Jalan Hospital, 47000 Sungai Buloh, Selangor, MALAYSIA

ABSTRACT

Bone fracture is the most common orthopedics problem. To achieve stability in the internal fixation of bone fragments, apply a Locking Compression Plate (LCP), which consists of a set of plates and screws. Common materials used for the bone fixation plate are stainless steel, titanium, and other metal alloys. Those materials are stiffer than cortical bone, causing a stress shielding effect. The stress shielding phenomenon takes place during bone remodelling, which affects the growth of bone and bone loss upon the healing process. The purpose of this study is to design the best LCP to minimize or eliminate the stress shielding issue for tibia shaft fracture. A reverse engineering process is used to obtain the solid part using 3D scanning, and data clean-up is done in CATIA V5, which is then used to be imported into the finite element software ANSYS 23R2. The fracture simulation is on transverse type fractures with the creation of a gap of 1 mm around the mid-tibial shaft region. Several boundary conditions will be parametrized, such as material properties, contact definitions, meshing, and loading conditions in preprocessing. This paper examines and simulates the behaviour of LCP under a load via finite element analysis (FEA). Design 2 was selected due to its superior stress distribution,

resulting in the LCP bearing only 177.98 MPa with a total deformation of 0.57 mm.

Keywords: *Stress Shielding; Locking Compression Plate (LCP); Finite Element Analysis (FEA)*

Introduction

Fractures of the long bone constitute one of the most prevalent injuries experienced by individuals during traumatic events, encompassing incidents ranging from sports-related injuries and vehicular accidents to falls [1]. Most of the time, the long bones affected by immense trauma are the tibial, humerus, ulna, and radius. The human skeleton consists of two primary types of bones: compact (cortical) bone which is characterized by density and hardness and also spongy (cancellous) bone, which is porous and lighter [2]. Bones undergo three consecutive phases like resorption, reversal, and formation [3].

Primary and secondary fracture healing are the two patterns of fracture healing [4]-[5]. Even though it rarely happens, primary healing terms directly refer to the cortex's effort to rebuild the bone itself after an interruption causing some displacements. Primary healing can only take place when the fracture fragments are anatomically reduced or achieve stability through rigid internal fixation, which affects interfragmentary strain to a micrometric level [6]. Whereas the most common fractures are healed by secondary healing, which entails adaptations in the periosteum and external soft tissues followed by the formation of a callus that will restore the fracture site to healing. Secondary healing is characterized by several distinct phases involving hematoma formation, callus buildup, callus hardening, and bone remodelling [7]. This healing process either takes months or even years, as the bone remodelling is crucial to developing fully functional bone.

In the case of bone fixation, especially for long bones, some alternative devices that have been developed to treat are plates, intermedullary rods, and external fixation [8]. Most of the time, the plate and screw method is usually used due to its mechanism, which minimizes the damage to the medullary canal like the use of intermedullary rods [9]-[10]. This could provide even faster recovery as the stem cells and the bone marrow damage are reduced. Even though the plate method takes less damage, some of the drawbacks that should be considered are the reduction of blood supply and the constrictions of callus formation since plates use the direct compression method to the bone, or so-called dynamic compression plate (DCP) [11]-[12]. Therefore, as an evolutionary step, the locking mechanism is introduced through LCP, which keeps a distance between bone and plates and induces a greater healing mechanism through effective callus formation [13]. Additionally, the plate can be angle adjusted to the bone, resulting in a bone that is near its original state.

Many researchers have explored ways to enhance the LCP, including the design and material applied [14]-[16]. This is seen when various plates have holes and forms that vary. Some plates are flat, while others have certain curvatures to fit the surface of the bone. Absolute stability is required for achieving primary healing experimentally, and less stability is required to achieve secondary healing. However, excessive interfragmentary instability will impede cartilage replacement, diminish angiogenesis, and prevent bone from bridging the fracture gap [17]. The current material options available include titanium alloys, stainless steel, and cobalt-chromium alloys, which are high-strength materials, which is the dominant cause of the stress shielding effect [8]. This effect prevents the generation and development of healed bone at the fracture site and may cause some severe osteoporosis and bone re-fracturing problems during the healing period [18]. The gap value of Young's modulus between the materials and the bone is huge. One of the primary causes of the stress shielding phenomenon, which is characterized by a lack of mechanical stimulation of the bone through an imbalance in load distribution throughout the bone plate build, is this significant disparity [19].

Stainless steel and titanium are commonly used materials for internal fixation due to their high Young's modulus [20]. However, after implantation, stress and strain can have negative effects on bone density, weakening the bone when subjected to loads. Unlike typical mechanical loading, the bone tissue experiences stress shielding, disrupting the distribution of load across the bone and disturbing bone remodelling [21]. This can lead to loosening of the implant and potential bone loss. To address this, reducing the rigidity of the fixation plate can promote more balanced load sharing between the plate and the bone while maintaining good primary fixation.

The objective of the study is to design an optimal LCP that offers both flexibility and strength via comparison of the results of FEA through the identification of Von Mises stress and total deformation of design.

Methodology

Several designs were made based on a literature review to find the best plate with optimal stiffness and strength. Due to the limitation of the study, a simple 3.5 mm type narrow plate had been obtained from the Hospital of UiTM, Sungai Buloh. Using this sample, the location of the hole can be mismatched with the catalog information through benchmarking Synthes 4.5 mm / 5 mm Narrow LCP with eight holes [22] with a referral catalog code of 224.581. CAD models with 8 holes were generated using CATIA V5R21 and later to .stp format, and data cleanup was done. The procedure was repeated for locking the head screw with referral model 213.336.

Preliminary model

Some design specifications of benchmark LCP, locking screw 5 mm, and tibia bone are gathered in Table 1.

Table 1: Modelling parameters of benchmark LCP, locking screw and tibia bone

Properties	Dimension
LCP	
Length	152 mm
Width	13.5 mm
Height	4.2 mm
Counter sunk hole (dynamic + locking)	8*(5 mm with height 2.5 mm + 6 mm with height 2.1 mm)
Locking screw 5 mm	
Shaft length	35 mm
Shaft diameter	5 mm
Thread pitch	1 mm
Screw head height	2.5 mm
Screw head diameter	7 mm
Tibia bone	
Length	351 mm

The generation of the new design was inspired by the benchmark to develop several designs of LCP and be compared in the morphological chart. In terms of the screw, 5 mm-diameter locking screws are created based on the product produced by the company Depuy Synthes, which fits relatively to the locking plate. Besides that, for a particular early stage of testing, a local CAD repository bone will be used and collected from GrabCAD and converted to .igs format. This allows for imitation of the study, which will be assembled purely in the Ansys Design modeler.
















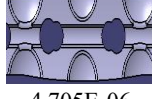
Design concept

The development of new designs will draw inspiration from established benchmarks, leading to the creation of several variations of LCP. These designs will be systematically compared and evaluated using a morphological chart as per Table 2 to determine the most effective configurations.

Specifically, the screw dimensions have been set at 5 mm for the locking screws, modelled based on the products produced by DePuy Synthes. This ensures a compatible fit with the locking plate, adhering to high standards of design and functionality. For the initial phase of testing, a local CAD repository bone model was sourced from GrabCAD. This model will be converted to .igs format to facilitate its integration and manipulation within the Ansys Design Modeler environment. The use of this local CAD repository

bone model will allow for an accurate imitation of real-world conditions, enabling comprehensive assembly and testing purely within the Ansys Design Modeler.

Table 2: Morphological chart of designs

View	Benchmark	Design 1	Design 2	Design 3
Holes				
Side				
Front				
Bottom				
Volume (m ³)	4.374E-06	4.878E-06	4.414E-06	4.705E-06

In the design featuring holes, all variations share identical information where each hole is precisely spaced 18.5 mm apart. Notably, in the side view, design 2 and design 3 exhibit slightly narrower 19 mm grooves encircling the middle section of the LCP, deviating from the consistent 20 mm grooves present in design 1 and the benchmark model. Moreover, design 1 stands out with a uniquely flat front surface, contrasting with the other designs that exhibit more uniform curvature characteristics. Additionally, a significant redesign is evident in design 3's undersurface profile, featuring a gutter-like surface that extends along the length of the LCP while the side of the LCP was thickened by 1 mm. This redesign incorporates a 1.25 mm fillet to mitigate sharp edges, enhancing both the aesthetic and functional aspects of the design.

Utilization of FEA for LCP fixation to tibial bone

Using ANSYS 23R2, various geometrical manipulations were performed to create a 1 mm fracture gap in a tibial diaphysis model. In a previous study, the tibial diaphysis was bisected to introduce a 1 mm gap, allowing for the simulation of callus bridging. This setup aimed to predict the behaviour response towards LCP under axial load at the tibia head.

During the creation of this gap, specific tools within the Design Modeler were employed, including the plane move and boolean functions as per Figure 1. These tools facilitated precise adjustments to the geometry, ensuring an accurate representation of the fracture. Additionally, for simplification

purposes, both ends of the tibia were horizontally cut. This modification ensured that force could be evenly applied through the tibial head while maintaining a static, fixed position at the other end. As a result of these manipulations, four distinct body segments were created, comprising both cancellous and cortical bone, each separated by a 1 mm transverse fracture gap. This setup was essential for the subsequent analysis of the mechanical and biological responses during the bone healing process under the applied compression load.

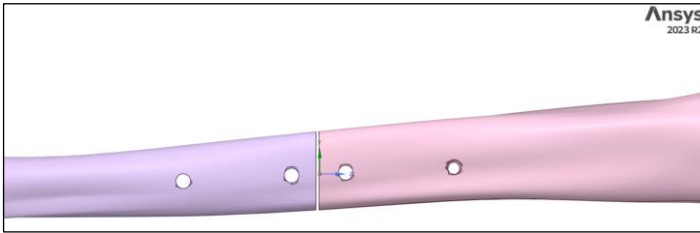


Figure 1: 1 mm gap bridging on tibial bone

Upon completing the gap bridging process, the LCP and the 5 mm locking head screws were imported from the CATIA V5 format into Ansys SpaceClaim as per Figure 2. Despite the complexity involved in placing the LCP and the 4 locking screws accurately, the manipulation process was meticulously handled. Placement of LCP is conducted at the anteromedial part of the tibia due to the fact that it reduces the damage of musculoskeletal tissue upon bending of the tibia which leads to the discomfort of the patient. Apart from that, a careful approach was crucial to ensure the homogeneous placement of the components in order to have a good comparison result. The integration of the LCP and screws required precise alignment to maintain the structural integrity and functionality of the fracture fixation. After that, some boundary conditions were applied in Figure 2, where the area of force applied to the tibia head was split into two regions, with one (A) pressing the left part of the bone and the other (C) pressing the right side of the tibia head. Fixed support was also introduced at the other end of the tibia bone to simulate the normal force on the ground.

Moving on to the preprocessing phase, it was crucial to establish boundary conditions and contact points to accurately simulate the tibial bone bending under a compression load applied at the tibial head. Key parameters included material properties, for which an elastic isotropic definition was applied in Ansys. Table 3 details the specific engineering parameters used, such as Young's modulus and Poisson's ratio, to ensure accurate material behaviour under stress.

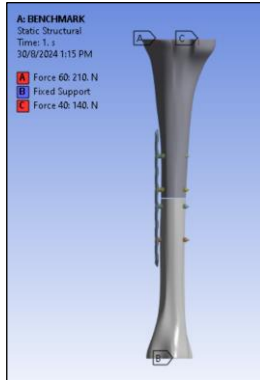


Figure 2: Full assembly LCP fixation device and tibial bone with boundary condition applied

Table 3: Materials properties

Materials	Young's modulus (Pa)	Poisson's ratio
Cortical bone [16]	1.62E+10	0.3
Cancellous bone [23]	2.1E+9	0.3
Stainless steel 316L [24]	1.95E+11	0.25

Boundary conditions were set by fixing one end of the tibia as a static reference point and applying a uniform compression load at the tibial head. Contact points between the bone segments, the LCP, and the screws were defined to accurately replicate load transfer and interactions. This careful preprocessing ensured reliable simulation results for the tibial bone's response under compression.

Results and Discussion

Von Mises stress

Finishing up the analysis from the previous FEA model based on several designs, several aspects were looked through, such as the Von Mises stress and the total deformation.

Figure 3 presents a contour plot illustrating the stress distribution of various LCP designs under axial compression. Each design's performance was evaluated by subjecting the tibial head to a load of 350 N that was split into a 60% and 40% region as referenced in [16]. The results indicate that Design 2 exhibited the lowest stress value, recording a stress of 177.98 MPa. This value corresponds to approximately 23.86% difference in the stress observed in the

benchmark model under identical loading conditions, which offer wider stress distributions.

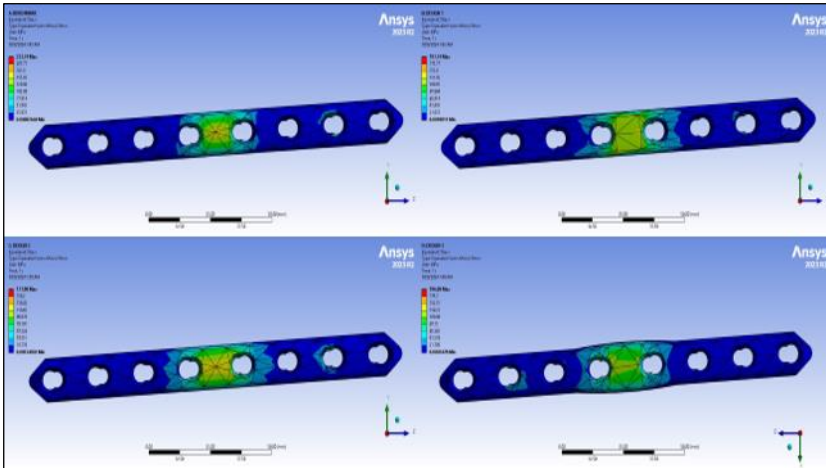


Figure 3: Contour plot Von Mises stress (MPa)

From Table 4, a significantly higher stress percentage value in Design 2 suggests an improved stress distribution compared to the benchmark model, even though it slightly possesses a higher volume, and vice versa with what happens in Design 1, as referred to in Table 5. Despite all models being subjected to the same 350 N axial load, Design 2 demonstrated superior performance in mitigating stress concentrations. These findings highlight the efficacy of Design 2 in enhancing load distribution across the tibial shaft, thereby potentially reducing the risk of mechanical failure or stress-related complications. Consequently, it can be inferred that Design 2 offers a more optimized structural configuration for stress management in orthopedic applications.

Table 4: Mechanical properties of each model

Model	Maximum Von Mises stress (MPa)	Percentage difference of Von Mises stress with benchmark model (%)	Factor of safety
Benchmark	233.74	0	1.24
Design 1	197.74	15.40 (decrease)	1.47
Design 2	177.98	23.86 (decrease)	1.63
Design 3	196.08	16.11 (decrease)	1.48

Displacement (mm)

Numerous researchers have employed displacement or so-called deformation metrics to evaluate and demonstrate the stability of various systems or constructs, as evidenced by studies [25]-[27]. Displacement measurements serve as a critical parameter in assessing the mechanical stability and performance of orthopedic implants and bone-plate systems.

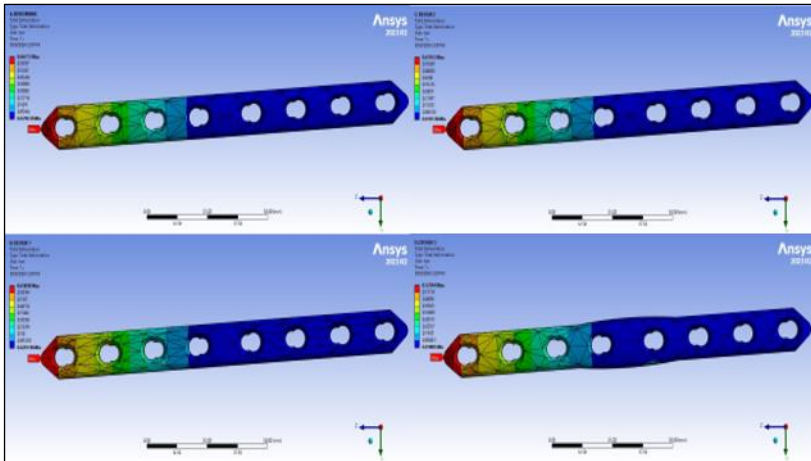


Figure 4: Contour plot total deformation (mm)

Total deformation in the context of LCPs refers to the movement or displacement of the plate under load, which indirectly affects the strain at the fracture site. While specific values for total deformation vary depending on the bone, fracture type, and LCP design, studies suggest that controlled micromotion in the range of 50 - 600 μm can promote callus formation [28]. The contour plot in Table 5 reveals the deviation from the benchmark value is within the range of suggested micromotions. This indicates that the observed variations are minimal and do not significantly diverge from the established benchmark.

Table 5: Total deformation indicator for stability of LCP

Model	Total deformation	
	millimetre, mm	micrometre, μm
Benchmark	0.6677	667
Design 1	0.6586	659
Design 2	0.6193	619
Design 3	0.57294	573

Design selection model

In selecting the optimal design, each criterion was rigorously analysed, as detailed in Table 6, to ensure a comprehensive evaluation from an engineering standpoint. The maximum stress value, which represents the highest stress concentration within the structure, was observed to occur at the Locking Compression Plate (LCP). Upon visual analysis, as illustrated in Figure 4, it was confirmed that Design 2 offers a score of 4, making it the lowest maximum stress. This was due to having the most efficient stress distribution compared to other configurations, making it the most effective shape for bearing loads. This efficient distribution is crucial for preventing localized failures and enhancing the overall durability and performance of the LCP.

Table 6: Decision matrix of design

Criterion	Benchmark	Rank/Score	Design 1	Rank/Score	Design 2	Rank/Score	Design 3	Rank/Score
Maximum stress (MPa)	233.74	Highest/1	197.74	High/2	177.98	Lowest/4	196.08	Low/3
Volume (m ²)	4.37E-06	Lowest/4	4.88E-06	Highest/1	4.41E-06	Low/3	4.71E-06	High/2
Shape deformation (mm)	0.67	Highest/1	0.66	Highest/1	0.62	Low/3	0.57	Lowest/4
Factor of safety	1.24	Lowest/1	1.47	High/2	1.63	Highest/4	1.48	High/3
Total		7		7		14		12

*Maximum stress (the lower the better), Volume (the lower the lighter), Shape deformation (the higher the lower), Factor of safety (the higher the better).

The volume criterion is an indicator of material usage that is most efficient in the benchmark, suggesting the lowest material and cost implications are small compared to the others. This is prior to the patient's comfort and manufacturing ability in future works. Based on the factor of safety in Equation (1), measuring the design's resilience to unexpected loads [29] using stainless steel 316L yield strength and maximum design stress values is crucial in determining the risk of failure for LCP. After some calculations, Design 2 is nominated as the safest and most robust option as it has the highest ratio value.

$$F.S = \frac{\sigma_Y}{\sigma} \tag{1}$$

In shape deformation, where a lower score indicates the least deformation under stress, is most favourable in Design 3. It is important to also take into consideration LCP deformation under stress, as it is an indicative measure of the stability of a structure that leads to its structural integrity. The

total score, reflecting an aggregate of these critical factors, places Design 2 at the highest (14.00), demonstrating its overall superior performance in stress distribution and safety, despite its second in place for volume and deformation scores. Thus, Design 2 emerges as the most advantageous choice, offering a balanced solution that meets stringent engineering requirements for performance, safety, and structural integrity, albeit with careful consideration of its higher material usage and deformation under load.

Conclusion

This study successfully identified the optimal LCP design by manipulating the topology and geometry of commercially available bone plates. Using CATIA V5R21, CAD models of the commercial plate from Synthes, along with several models from previous studies, were developed. Each of the designs was thoroughly analysed in Ansys 23R2, and the result is that Design 2 emerged as the most promising configuration. Future research could explore the implementation of composite materials with Design 2 to further enhance its performance and potential clinical applications.

Contribution of Authors

Muhammad Naufal Nazeri: Conceptualization, Data collection, Simulation, Data analysis, Writing draft. Solehuddin Shuib: Funding acquisition, review and editing. Ahmad Zafir Romli: Material preparation. Mohd Fairudz Mohd Miswan: medical implant consultation.

Funding

This work was supported by the FRGS scheme with project number 600-RMC/FRGS 5/3 (003/2023).

Conflict of interest

All authors declare that they have no competing interests.

Acknowledgement

Authors acknowledge the Ministry of Higher Education (MOHE) for funding under the Fundamental Research Grant Scheme (FRGS) (FRGS/1/2023/TK10/UITM/01/1). Additionally, we would like to express our sincere gratitude to the College of Engineering, UiTM Shah Alam, for their invaluable support and guidance throughout our academic journey.

References

- [1] N. S. Anandasivam G. S. Russo, M. S. Swallow, B. A. Basques, A. M. Samuel, N. T. Ondeck, S. H. Chung, J. M. Fischer, D. D. Bohl, and J. N. Grauer, "Tibial shaft fracture: A large-scale study defining the injured population and associated injuries," *Journal of Clinical Orthopaedics and Trauma*, vol. 8, no. 3, pp. 225–231, 2017. doi: 10.1016/j.jcot.2017.07.012
- [2] Y. Su, C. Luo, Z. Zhang, H. Hermawan, D. Zhu, J. Huang, Y. Liang, G. Li, and L. Ren, "Bioinspired surface functionalization of metallic biomaterials," *Journal of the Mechanical Behavior of Biomedical Materials*, vol. 77, pp. 90–105, 2018. doi: 10.1016/j.jmbbm.2017.08.035
- [3] D. J. Hadjihakis and I. I. Androulakis, "Bone remodeling", *Annals of the New York Academy of Sciences*, vol. 1092, no. 1, pp. 385–396, 2006. doi: 10.1196/annals.1365.035
- [4] H. Elhawary, A. Baradaran, J. Abi-Rafeh, J. Vorstenbosch, L. Xu, and J. I. Efanov, "Bone healing and inflammation: principles of fracture and repair", *Seminar in Plastic Surgery*, vol. 35, no. 03, pp. 198–203, 2021. doi: 10.1055/s-0041-1732334
- [5] N. S. Makaram, A. Param, N. D. Clement, and C. E. H. Scott, "Primary versus secondary total knee arthroplasty for tibial plateau fractures in patients aged 55 or over—A systematic review and meta-analysis," *The Journal of Arthroplasty*, vol. 39, no. 2, pp. 559–567, 2024. doi: 10.1016/j.arth.2023.08.016
- [6] R E Kaderly, "Primary bone healing", *Seminar Veterinar Medical Surgical Small Animal*, vol. 6, no. 1, pp. 5–21, 1991.
- [7] T. A. Einhorn and L. C. Gerstenfeld, "Fracture healing: mechanisms and interventions", *Nature Reviews Rheumatology*, vol. 11, no. 1, pp. 45–54, 2015. doi: 10.1038/nrrheum.2014.164
- [8] V. Verma and K. Pal, "A finite element investigation on the design of mechanically compatible functionally graded orthopaedic plate for diaphyseal tibia transverse fracture", *Composites Part C: Open Access*, vol. 7, pp. 1-11, 2022. doi: 10.1016/j.jcomc.2022.100228
- [9] R. J. Brumback and W. W. Virkus, "Intramedullary Nailing of the Femur: Reamed Versus Nonreamed," *Journal of the American Academy of*

- Orthopaedic Surgeons*, vol. 8, no. 2, pp 83-90, 2000, [Online]. Available: https://journals.lww.com/jaaos/fulltext/2000/03000/intramedullary_nailing_of_the_femur_reamed_versus.2.aspx/ (Accessed).
- [10] T. Yamanaka, T. Matsumura, R. Ae, S. Hiyama, and K. Takeshita, “Risk of peri implant femoral fracture after cephalomedullary nailing in older patients with trochanteric fractures”, *Injury*, vol. 55, no. 6, pp. 1-6, 2024. doi: 10.1016/j.injury.2023.111206
- [11] S. M. Perren, K. Mane, O. Pohler, M. Predieri, S. Steinemann, and E. Gautier, “The limited contact dynamic compression plate (LC-DCP)”, *Archives of Orthopaedic and Trauma Surgery*, vol. 109, no. 6, pp. 304–310, 1990. doi: 10.1007/BF00636166
- [12] H. Wee, J. Staub, Z. Koroneos, A. Kunselman, J. S. Reid, and G. S. Lewis, “Mechanics of dynamic compression plate application in fracture fixation”, *Clinical Biomechanics*, vol. 113, pp. 1-7, 2024. doi: 10.1016/j.clinbiomech.2024.106209
- [13] R. Frigg, “Development of the locking compression plate,” *Injury*, vol. 34, pp. 6–10, 2003. doi: 10.1016/j.injury.2003.09.020
- [14] M. S. A. Sulong, A. Syahrom, and Z. Zakaria, “Study of locking compression plate through biodegradable implant,” *Journal of Medical Device Technology*, vol. 1, no. 1, pp. 56–63, 2022. doi: 10.11113/jmeditec.v1n1.18
- [15] A. Mehboob and S.-H. Chang, “Effect of composite bone plates on callus generation and healing of fractured tibia with different screw configurations”, *Composites Science and Technology*, vol. 167, pp. 96–105, 2018. doi: 10.1016/j.compscitech.2018.07.039
- [16] M. K. A. Suaimi, A. M. A. Rashid, A. K. Nasution, G. H. Seng, M. R. A. Kadir, and M. H. Ramlee, “Biomechanical evaluation of locking compression plate (LCP) versus dynamic compression plate: A finite element analysis,” *Jurnal Teknologi*, vol. 84, no. 3, pp. 125–131, 2022. doi: 10.11113/jurnalteknologi.v84.16687
- [17] J. Li, L. Qin, K. yang, Z. Ma, Y. Wang, L. Cheng, and D. Zhao, “Materials evolution of bone plates for internal fixation of bone fractures: A review,” *Journal of Material Science and Technology*, vol. 36, pp. 190–208, 2020. doi: 10.1016/j.jmst.2019.07.024
- [18] A. Kabiri, G. Liaghat, and F. Alavi, “Biomechanical evaluation of glass fiber/polypropylene composite bone fracture fixation plates: Experimental and numerical analysis,” *Computers in Biology and Medicine*, vol. 132, pp. 1-16, 2021. doi: 10.1016/j.compbiomed.2021.104303
- [19] A. A. Al-Tamimi, “3D topology optimization and mesh dependency for redesigning locking compression plates aiming to reduce stress shielding,” *International Journal of Bioprinting*, vol. 7, no. 3, pp. 153-162, 2021. doi: 10.18063/ijb.v7i3.339

- [20] D. Aroussi, B. Aour, and A. S. Bouaziz, “A comparative study of 316l stainless steel and a titanium alloy in an aggressive biological medium”, *Engineering, Technology and Applied Science Research*, vol. 9, no. 6, pp. 5093–5098, 2019. doi: 10.48084/etasr.3208
- [21] W. Xiong, X. Ding, H. Zhang, T. Hu, S. Xu, P. Duan, and B. Huang, “Topology optimization of embracing fixator considering bone remodeling to mitigate stress shielding effect”, *Medical Engineering and Physics*, vol. 125, no. 10, pp. 104-122, 2024. doi: 10.1016/j.medengphy.2024.104122
- [22] De Puy Synthes, “Large Fragment LCP® Instrument and Implant Set Surgical Technique” [Online]. Available: <https://synthes.vo.llnwd.net/o16/LLNWMB8/US%20Mobile/Synthes%20North%20America/Product%20Support%20Materials/Technique%20Guides/DSUSTRM09161038%20Rev%20C.pdf/> (Accessed: May 25, 2024).
- [23] D. Wu, P. Isaksson, S. J. Ferguson, and C. Persson, “Young’s modulus of trabecular bone at the tissue level: A review”, *Acta Biomaterialia*, vol. 78, pp. 1–12, 2018. doi: 10.1016/j.actbio.2018.08.001
- [24] Z. Zhang, T. Yu, L. Xie, Y. Li, X. Ke, Y. Liu, S. Huang, H. Deng, and Y. Bai, “Biomechanical bearing based typing method for osteonecrosis of the femoral head: ABC typing”, *Experimental and Therapeutic Medicine*, vol. 16, no. 3, pp. 2682-2688, 2018. doi: 10.3892/etm.2018.6488
- [25] D. Jiang, S. Zhan, Q. Wang, M. Ling, H. Hu, and W. Jia, “Biomechanical comparison of locking plate and cancellous screw techniques in medial malleolar fractures: a finite element analysis,” *The Journal of Foot and Ankle Surgery*, vol. 58, no. 6, pp. 1138–1144, 2019. doi: 10.1053/j.jfas.2018.10.005
- [26] J.-J. Zhou, M. Zhao, D. Liu, H.-Y. Liu, and C.-F. Du, “Biomechanical property of a newly designed assembly locking compression plate: Three-dimensional finite element analysis,” *Journal of Healthcare Engineering*, vol. 2017, no. 2, pp. 1–10, 2017. doi: 10.1155/2017/8590251
- [27] M. H. Ramlee, M. A. Sulong, E. Garcia-Nieto, D. A. Penaranda, A. R. Felip, and M. R. A. Kadir, “Biomechanical features of six design of the delta external fixator for treating Pilon fracture: A finite element study”, *Medical and Biological Engineering and Computing*, vol. 56, no. 10, pp. 1925–1938, 2018. doi: 10.1007/s11517-018-1830-3
- [28] C. Ma, T. Du, X. Niu, and Y. Fan, “Biomechanics and mechanobiology of the bone matrix”, *Bone Research*, vol. 10, no. 1, p. 59, 2022. doi: 10.1038/s41413-022-00223-y
- [29] H. Santana, D. Parco, C. Galdos, A. Calcina, R. De la Cruz, and N. Moggiano, “Design of 10:1 speed reducer for an elevator,” *Journal of Physics Conference Series*, vol. 2512, no. 1, pp. 12-11, 2023. doi: 10.1088/1742-6596/2512/1/012011